

Cross Wind Effects on Fire Propagation through Heterogeneous Media

B. Porterie¹, D. Morvan², J.C. Loraud¹ and M. Larini¹

¹ IUSTI UMR CNRS 6595

5 rue E. Fermi, Technopôle de Château-Gombert, 13453 Marseille cedex 13 FRANCE

e-mail: berni@iusti.univ-mrs.fr

² IRPHE UMR CNRS 6594

60 rue J. Curie, Technopôle de Château-Gombert, 13453 Marseille cedex 13 FRANCE

ABSTRACT

A two-phase formulation is used to study the cross wind effects on the propagation of a line fire through a fuel bed. Each phase is described by a set of time-dependent equations and the coupling between them is rendered through exchange terms of mass, momentum, and energy. Turbulence is approached by using a RNG (Renormalization Group) $k - \epsilon$ statistical model. The radiative transfer equation in the fuel bed is solved using the discrete ordinates method extended to a two-phase medium. Soot formation is considered. First-order kinetics is incorporated to describe pyrolysis and combustion processes. A finite-volume method including high-order upwind convective scheme and flux limiter strategy along with a projection method for the pressure-velocity coupling is used. The effects of cross wind on the behaviour of a line fire through a bed of pine needles are examined and compared to measurements.

KEYWORDS: Fire dynamics, multiphase flow, heterogeneous media, wind-driven fire.

INTRODUCTION

Following Weber [1], the various mathematical models for predicting the rate of spread (ROS) of a wildland fire can be classified as statistical, empirical, and physical models according to whether they involve no physics at all, no distinction between different modes of heat transfer, or account for each mechanisms of heat transfer individually. The purpose of these models is mainly restricted to the prediction of the ROS. Among the physical models, the model of Grishin *et al.* [2] is the first model to incorporate kinetics to describe pyrolysis and combustion but it does not account for hydrodynamics. A new development of physical models appeared in 1985 with the pioneering work of Grishin *et al.* [3] insofar as they describe the hydrodynamics through the fuel matrix and above the fuel bed by using a two-phase approach. These models not only can predict the ROS of the fire but also its complete behaviour. In the work of Grishin *et al.* [3], thermal equilibrium between the gas phase and one solid phase is assumed and the formulation is simplified by averaging the equations over the height of the forest canopy. The aim of the present work is to study the effects of a cross wind on the ROS of a line fire through an heterogeneous medium by using a complete two-phase physical model in which the phases are in thermal non equilibrium. Each phase is modelled by a set of time-dependent equations coupled together through exchange terms of mass, momentum, and energy. Turbulence, radiation, and soot formation are considered for improving physical insight. Wind effects on the unsteady development of the fire are examined. Computed ROS are only compared to laboratory measurements. It is worthy of note that our model could be used whatever the scale, but due to the lack of data on large-scale fires, its validity is only demonstrated on small-scale

experiments. On the other hand, the extension of our model to simulate three dimensional phenomena is not problematic from a theoretical point of view but it would be prohibitively expensive and very time consuming. A strategy based on parallel computing seems to be a well-adapted alternative. In addition, for the sake of simplicity, particles are fixed in space and time. That means that, at this stage of development, our model cannot handle the dispersion of flying particles, such as burning brands which can cause spotting ahead of the fire.

ANALYSIS

Let us consider a small control volume V in which a solid phase and a gas phase coexist. The solid-phase volume fraction is defined as $\alpha_s = V_s/V$ where V_s is the volume occupied by the solid phase s in the volume V . In the same way, the gas volume fraction is defined as $\alpha_g = V_g/V$. From these definitions, we have $\alpha_g + \alpha_s = 1$. Transfers between phases are the key concept for the understanding of fire propagation mechanisms. These transfers are directly related to the specific wetted area A_s , expressed as follows

$$A_s = \tilde{n}_s s_s = V_s \frac{\tilde{n}_s s_s}{V_s} = \frac{V_s}{V} \frac{s_s}{v_s} = \alpha_s \sigma_s \quad (1)$$

where $\sigma_s = s_s/v_s$ is the surface to volume ratio of a solid particle, \tilde{n}_s the number density (number of particles per unit volume). For each phase a set of time-dependent equations based on the laws of conservation of mass, momentum, chemical species, energy is derived. Because of density variations due to combustion heat release, the present multicomponent turbulent reactive flow is formulated using the Favre density-weighted averaging approach. By assuming that thermal and species diffusivities are equal, the average mass, momentum, energy, and species conservation equations may be written as

$$\frac{\partial \bar{p}}{\partial t} + \frac{\partial}{\partial x_j} (\bar{p} \tilde{u}_j) = [\dot{M}]_I \quad (2)$$

$$\frac{\partial}{\partial t} (\bar{p} \tilde{u}_i) + \frac{\partial}{\partial x_j} (\bar{p} \tilde{u}_j \tilde{u}_i) = \frac{\partial \bar{\sigma}_{ij}}{\partial x_j} - \frac{\partial \overline{\rho u_j u_i}}{\partial x_j} + \bar{p} g_i - [F_i]_I \quad (3)$$

$$\begin{aligned} \frac{\partial}{\partial t} (\bar{p} \tilde{h}) + \frac{\partial}{\partial x_j} (\bar{p} \tilde{u}_j \tilde{h}) &= \frac{\partial}{\partial x_j} \left(\frac{\bar{\mu}}{Pr} \frac{\partial \tilde{h}}{\partial x_j} \right) + \frac{\partial \bar{p}}{\partial t} - \frac{\partial \overline{\rho u_j h}}{\partial x_j} - \frac{\partial q_j^R}{\partial x_j} \\ &\quad - [Q_{cond}]_I + [\dot{M}h]_I \end{aligned} \quad (4)$$

$$\frac{\partial}{\partial t} (\bar{p} \tilde{Y}_\alpha) + \frac{\partial}{\partial x_j} (\bar{p} \tilde{u}_j \tilde{Y}_\alpha) = \frac{\partial}{\partial x_j} \left(\frac{\bar{\mu}}{Pr} \frac{\partial \tilde{Y}_\alpha}{\partial x_j} \right) - \frac{\partial \overline{\rho u_j Y_\alpha}}{\partial x_j} + \bar{\omega}_\alpha + [\dot{M}Y_\alpha]_I \quad (5)$$

where $\rho = \alpha_g \rho_g$, $p = \alpha_g p_g$, and $\mu = \alpha_g \mu_g$

The subscript g refers to gas properties, the superscripts $(-)$, $(\tilde{\quad})$, and $(\overline{\quad})$ denote time average, density-weighted Favre average and density-weighted Favre fluctuation. In these equations, ρ , μ , u_i , h , Y_α , p , q_i^R , g_i , ω_α are the density, viscosity, velocity component in the direction i , enthalpy, mass fraction of species α , pressure, radiative heat flux and gravity acceleration component in the direction i , and the rate of production of species α , respectively. $Pr = \mu_g C_p / \lambda$ is the average Prandtl number where λ is the thermal conductivity of the gas and $C_p = \sum_\alpha Y_\alpha C_{p\alpha}$ the constant-pressure specific heat of the gas mixture.

The average stress tensor is approximated as

$$\bar{\sigma}_{ij} = -\bar{p} \delta_{ij} + \bar{\mu} \left(\frac{\partial \tilde{u}_i}{\partial x_j} + \frac{\partial \tilde{u}_j}{\partial x_i} - \frac{2}{3} \frac{\partial \tilde{u}_k}{\partial x_k} \delta_{ij} \right) \quad (6)$$

where δ_{ij} is the Kronecker delta.

Mixture static enthalpy is defined to include the chemical energy.

The equation of state for a multicomponent system based upon ideal-gas assumptions can be written as

$$p = \rho RT \sum_\alpha \frac{Y_\alpha}{W_\alpha} \quad (7)$$

The gaseous phase viscosity depends on temperature.

The terms between brackets with subscript I in the conservation equations correspond to mass, momentum and energy transfers at the interface between the gas and the solid phase.

The turbulent fluxes in the momentum, energy and species conservation equations can be approximated from the Boussinesq's eddy viscosity concept and the generalized gradient diffusion assumption

$$-\overline{\rho u_j^n u_i^n} = \mu_t \left(\frac{\partial \tilde{u}_i}{\partial x_j} + \frac{\partial \tilde{u}_j}{\partial x_i} \right) - \frac{2}{3} \left(\mu_t \frac{\partial \tilde{u}_k}{\partial x_k} + \bar{\rho} k \right) \delta_{ij} \quad (8)$$

$$-\overline{\rho u_j^n \phi^n} = \frac{\mu_t}{\sigma_\phi} \frac{\partial \phi}{\partial x_j} \quad (9)$$

where σ_ϕ is the turbulent Prandtl/Schmidt number for ϕ .

The eddy viscosity μ_t is evaluated from the turbulent kinetic energy k and its dissipation rate ε using the classical relation

$$\mu_t = \bar{\rho} C_\mu \frac{k^2}{\varepsilon} \quad (10)$$

Transport equations for k and ε can be obtained from the Renormalization Group theory (RNG) [4][5][6]

$$\frac{\partial}{\partial t} (\bar{\rho} k) + \frac{\partial}{\partial x_j} (\bar{\rho} \tilde{u}_j k) = \frac{\partial}{\partial x_j} \left[\left(\bar{\mu} + \frac{\mu_t}{\sigma_k} \right) \frac{\partial k}{\partial x_j} \right] + P_k + W_k - \bar{\rho} \varepsilon \quad (11)$$

$$\begin{aligned} \frac{\partial}{\partial t} (\bar{\rho} \varepsilon) + \frac{\partial}{\partial x_j} (\bar{\rho} \tilde{u}_j \varepsilon) &= \frac{\partial}{\partial x_j} \left[\left(\bar{\mu} + \frac{\mu_t}{\sigma_\varepsilon} \right) \frac{\partial \varepsilon}{\partial x_j} \right] + \\ &\frac{\varepsilon}{k} (C_{\varepsilon 1} P_k + C_{\varepsilon 3} W_k) - R P_k \frac{\varepsilon}{k} - C_{\varepsilon 2} \bar{\rho} \frac{\varepsilon^2}{k} \end{aligned} \quad (12)$$

where P_k and W_k are respectively the shear and buoyancy turbulent production/destruction terms

$$P_k = -\overline{\rho u_j^n u_i^n} \frac{\partial \tilde{u}_i}{\partial x_j} \quad W_k = -\frac{\mu_t}{\bar{\rho}^2} \frac{\partial \bar{\rho}}{\partial x_j} \frac{\partial \bar{p}}{\partial x_j} \quad R = \frac{\eta(1 - \eta/\eta_0)}{1 + \beta\eta^3}$$

$$\eta = \sqrt{\frac{P_k}{\bar{\rho} C_\mu \varepsilon}} \quad \eta_0 = 4.38 \quad \beta = 0.015 \quad C_\mu = 0.0845$$

$$C_{\varepsilon 1} = 1.42 \quad C_{\varepsilon 2} = 1.68 \quad C_{\varepsilon 3} = 1.5 \quad \sigma_k = 0.7179 \quad \sigma_\varepsilon = 1.3$$

As suggested by Grishin *et al.* [7], the composition of the pyrolysis products is complicated (C , CO , CO_2 , H_2O , CH_4 , H_2 , C_2H_6 ...), and one of the most representative components is CO . Therefore, the kinetic scheme is simplified by assuming that pyrolysis products are effective gas of the CO type. To calculate the turbulent combustion, the Eddy Dissipation Concept (EDC) by Magnussen and Hjertager [8] is used. At the present stage, we have assumed fast chemistry for wildland fire calculations. That means that the local reaction rate is taken to be the slowest of the turbulence dissipation rates of either fuel, oxygen or hot products. Then, the mass rate of production of gaseous species due to the above reaction can be easily determined from

$$\dot{\omega}_{CO} = -A \bar{\rho} \frac{\varepsilon}{k} \min \left(\tilde{Y}_{CO}, \frac{\tilde{Y}_{O_2}}{s_2}, \frac{B \tilde{Y}_{CO_2}}{1 + s_2} \right), \dot{\omega}_{O_2} = s_2 \dot{\omega}_{CO}, \dot{\omega}_{CO_2} = -(1 + s_2) \dot{\omega}_{CO} \quad (13)$$

where $A = 4$, $B = 0.5$, and s_2 is the stoichiometric ratio of the chemical reaction



Concerning the solid phase, the mass balance equation can be written as

$$\frac{\partial}{\partial t} (\alpha_s \rho_s) = - [\dot{M}]_I \quad (15)$$

The rate of particle mass reduction relative to the thermal degradation of the solid fuel can be represented by the sum of the mass rates \dot{m}^{H_2O} , \dot{m}^{pyr} , \dot{m}^{char} , and \dot{m}^{ash} due to water vaporization, pyrolysis, char combustion (as a consequence of pyrolysis), and ash formation (as a consequence of char oxidation), respectively

$$[\dot{M}]_I = \dot{m}^{pyr} + \dot{m}^{H_2O} + \dot{m}^{char} + \dot{m}^{ash} \quad (16)$$

where

$$\dot{m}^{H_2O} = R^{H_2O}, \dot{m}^{pyr} = R^{pyr}, \dot{m}^{char} = -p^{char} R^{pyr} + R^{char}, \dot{m}^{ash} = -\frac{p^{ash}}{p^{char}} R^{char}$$

where p^{char} and p^{ash} are the char and ash contents of the solid fuel.

The rates of mass loss due to drying, pyrolysis, and char oxidation are deduced from Arrhenius-type laws. The kinetic parameters of the rate of pyrolysis of pine needles are determined by thermogravimetric analysis whilst those due to water vaporization and char oxidation are given by Grishin *et al.* [7]

$$R^{H_2O} = 6.10^5 T_s^{-\frac{1}{2}} m^{H_2O} \exp(-6000/T_s) \quad (17)$$

$$R^{pyr} = 3.63 \cdot 10^4 m^{pyr} \exp(-9400/T_s) \quad (18)$$

$$R^{char} = \frac{1}{s_1} 430 A_s \rho_{O_2} \exp(-9000/T_s) \quad (19)$$

where s_1 the stoichiometric ratio of the heterogeneous reaction.

Char is here idealized as pure carbon and the heterogeneous reaction is assumed to be



Particles are assumed to be fixed in time and space. So, the assumption of motionless particles serves as momentum equations for the solid phase: $u_s = v_s = 0$.

By considering the assumption that fuel particles are thermally thin, i.e. the temperature throughout any solid particle is uniform while it is being heated, the solid-phase heat-conduction equation reduces to

$$\alpha_s \rho_s C_{ps} \frac{\partial T_s}{\partial t} = -R^{pyr} L^{pyr} - R^{char} L^{char} - R^{H_2O} L^{H_2O} + [Q_{cond}]_I + [Q_{rad}]_I \quad (21)$$

where the specific heat of the solid phase, C_{ps} , is deduced from those of water and dry material, and the fractional mass moisture of the fuel material.

$[Q_{cond}]_I$ represents the conductive/convective energy flux between the gas and the solid phase, $[Q_{rad}]_I$ represents the net radiative energy flux at the surface of the solid phase.

Water vaporization and pyrolysis are endothermic processes ($L^{H_2O} = 2.25 \times 10^6 J/kg$ and $L^{pyr} = 418 J/kg$) whilst char combustion is highly exothermic ($L^{char} = -1.2 \times 10^7 J/kg$).

Soot formation is described through the evolution of the average soot volume fraction \tilde{f}_v accounting for oxidation process

$$\frac{\partial}{\partial t} (\tilde{\rho} \tilde{f}_v) + \frac{\partial}{\partial x_j} [\tilde{\rho} (\tilde{u}_j + \tilde{u}_j^{th}) \tilde{f}_v] = \frac{\partial}{\partial x_j} \left(\frac{\tilde{\mu}_t}{\sigma_f} \frac{\partial \tilde{f}_v}{\partial x_j} \right) + \overline{\omega}_{fv} \quad (22)$$

where \tilde{u}_j^{th} is the mean thermophoretic velocity components given by [9]

$$\tilde{u}_j^{th} = -0.54 \frac{\tilde{\mu}}{\tilde{\rho}} \frac{\partial \ln \tilde{T}}{\partial x_j}$$

In accordance with Grishin [10], we can assume that for the most part soot forms as a result of the pyrolysis of wildland fuels, and not of the decomposition of hydrocarbons in the gas phase. Then the source term $\overline{\omega}_{fv}$ takes the form

$$\overline{\omega}_{fv} = \frac{\tilde{\rho}}{\rho_{soot}} \left(\alpha_6 \dot{m}^{pyr} - \frac{6 \tilde{f}_v}{d_{soot}} W_{NSC} \right) \quad (23)$$

where $0.001 \leq \alpha_6 \leq 0.03$ is the percentage of pyrolysis products which corresponds to soot particle removal. The value used in the present calculations is: $\alpha_6 = 0.01$. The last term corresponds to the Nagle and Strickland-Constable (NSC) rate for oxidation by O_2 given in detail in [9]. This oxidation model needs the knowledge of the soot particle diameter d_{soot} . A typical value of $10 \mu m$ has been retained.

Radiation is considered assuming that the physical domain contains absorbing-emitting gray medium. By applying the multiphase approach, the radiative heat source which appears in the energy equation of the gas phase is given by

$$\frac{\partial q_j^R}{\partial x_j} = \alpha_g a_g \left(G - \frac{\sigma T^4}{\pi} \right) \quad (24)$$

The average incident radiation is expressed as

$$G = \int_{4\pi} L(\vec{\Omega}) d\Omega \quad (25)$$

where $L(\vec{\Omega})$ is the radiative intensity in the direction $\vec{\Omega}$ which can be obtained by solving the multiphase RTE

$$\Omega_j \frac{\partial}{\partial x_j} (\alpha_g L) = \alpha_g a_g \left(\frac{\sigma T^4}{\pi} - L \right) + \alpha_s a_s \left(\frac{\sigma T_s^4}{\pi} - L \right) \quad (26)$$

Since the homogeneous fuel bed can be approximated as optically thick, a simple radiation model could be used for describing radiative transfer within the fuel bed (see for example [11]). Nevertheless to correctly evaluate radiation from the flame to the fuel bed and to prepare future works on discontinuous media, an extension of the Discrete Ordinates Method (DOM) to multiphase media has been developed. DO solutions can be obtained using S_n approximations. That means that radiation calculations are based on solving the RTE in $M = n(n+2)$ discrete solutions ($M/2$ in case of 2D domain) to which is attached a set of weights. In the current study, we have retained the S_8 approximation ($M = 80$) and the ordinates directions and quadratic weighting factors (μ_m, ξ_m, w_m) have been taken from the works of Fiveland [12]. Eq. 26 is integrated over a control volume for each specified ordinate direction. The Variable Weighted scheme of Lathrop [13] is used to relate the facial intensities at the boundary of control volume to the cell center intensity.

The media properties are given by the absorption coefficients a_g and a_s for the gas and the solid phase, respectively. As mentioned by De Mestre *et al.* [14], the absorption coefficient a_s can be calculated from the standard formula (Committee on Fire Research, 1961): $a_s = A_s/4$.

Following Kaplan *et al.* [9], the absorption coefficient of the soot/combustion products (CO_2, H_2O) mixture is evaluated by assuming gray gas assumption from the mole fraction of the combustion products and the average soot volume fraction

$$a_g = 0.1(X_{CO_2} + X_{H_2O}) + 1862.f_v T(m^{-1})$$

The average incident radiation can be approximated by $G = \sum_{m=1}^M w_m L_m$ where w_m are the weights of the quadrature set.

In a similar manner, the radiation flux in the energy equation of the solid phase is

$$[Q_{rad}]_I = \alpha_s a_s (G - 4\sigma T_s^4) \quad (27)$$

The drag force per unit volume acting on the solid-phase particles can be expressed

$$[\mathbf{F}]_I = \frac{1}{8} A_s C_{D_s} \rho |\mathbf{u}| \mathbf{u} \quad (28)$$

The particle drag coefficient C_{D_s} depends on the Reynolds number Re_{es} of the solid phase based on the equivalent spherical radius of the particle. For the present calculations, the correlation proposed in [15] valid for spheres at $Re_{es} \leq 800$ is adopted

$$C_{D_s} = \frac{24}{Re_{es}} (1 + 0.15 Re_{es}^{0.687}) \quad (29)$$

The interphase convective/conductive heat flux is defined as

$$[Q_{cond}]_I = A_s h_s (T - T_s) \quad (30)$$

The heat transfer coefficient h_s is deduced from the correlation of Incropera and De Witt [16] for cylinders as $h_s = 0.5\lambda/r_s (0.683 Re_s^{0.466})$ where the Reynolds number Re_s is based on the radius of the cylindrical particle.

NUMERICAL METHOD

The governing equations are discretized on a staggered non-uniform grid using a finite-volume procedure with a high-order upwind scheme (Quick) for the convective terms [17] and a 2nd order backward Euler scheme for time discretization. A universal flux limiter DWF (Downwind Weighting Factor) is applied in conjunction with the Quick scheme to eliminate any possibility of overshoot or oscillation sometimes introduced by the convective schemes when the monotonicity of the solution is not ensured. The pressure-velocity coupling is treated using a projection method.

The resulting systems of linear algebraic equations for each variable are then solved iteratively using a TDMA algorithm [18]. In addition, to procure convergence and prevent low-frequency behaviour of the solution typical of this type of buoyancy-driven flow [19], all the variables were under-relaxed using inertial relaxation [18].

Different grids were tested to ensure that the solution was independent of the grid density. A grid size of 140x40 cells has been used for all of the cases solved. The time step is 0.01s.

RESULTS AND DISCUSSION

The behaviour of a spreading wildfire through a litter of dead pine needles (*Pinus Pinaster*) is simulated. A computational domain of 0.9m high and 4.2m long was used in accordance with the test conditions of laboratory experiments conducted by Ventura and Mendes-Lopes [20] in a wind tunnel. For a fuel load value of 0.5kg/m^2 , three wind speed values (1, 2, and 3m/s) were selected. The measured surface-to-volume ratio and density of the needles were respectively 551m^{-1} and 680kg/m^3 . The initial moisture content is around 10%. The fuel is distributed uniformly from 1 to 3.2m from the left boundary of the computational domain over a depth of 0.05m. The line fire is ignited at the left end of the fuel bed over a distance of 0.1m and over the whole depth. In this ignition zone, the fuel temperature varies linearly from 400K to 900K until 10s. Computations are stopped when the front of pyrolysis has reached 2.6m. Fig. 1 shows the time evolution of the gas temperature field and velocity vector for a cross wind of 1m/s. The diagrams reveal the unsteady stages of the wildfire propagation and the development of a strong buoyant plume. The upward movement of the flame gases is mainly due to buoyancy effects as usually observed in natural fires. The low momentum flowrate of the fuel vapor due to pyrolysis has no significant effect on flame behaviour which explains its non ordered structure. Moreover, the shear forces induce instability in the gas flow which leads to flame flickering.

The gas and solid phase temperature fields and velocity vector at $t=107\text{s}$ are shown in Fig. 2. The maximum in temperature is obtained in the region where char combustion occurs while that of gas temperature is observed in the intense pyrolysis region. This confirms the necessity to account for thermal non-equilibrium between the phases. In Fig. 3, the trajectory of the pyrolysis front is plotted for the three selected wind values. The predicted ROS compares reasonably well with the measured values (Fig. 4).

CONCLUSIONS

We first of all developed a 2D two-phase reactive model, involving turbulence, radiation, and soot formation, for the unsteady behaviour of a fire front spreading under windy conditions. It accounts for the hydrodynamics aspects of the flow, the basic physicochemical processes of thermal degradation (heating, drying, pyrolysis, and combustion) and uses first-order Arrhenius kinetics to describe thermal degradation and combustion. We compared the theoretical ROS with those observed in laboratory conditions. The agreement is qualitatively good and reveals a faithful reproduction of cross wind effects on the ROS. Studies about the sensitivity of ROS to the interphase drag along with large-scale investigations are now in progress.

ACKNOWLEDGMENT

The European Economic Commission is gratefully acknowledged for providing partial funding for this research in the frame of the EFAISTOS Project.

References

- [1] Weber, R.O., "Modelling Fire Spread through Fuel Beds", Prog. in Energy and Combust. Sci., 17, 67-82, 1991.
- [2] Grishin, A.M., Gruzin, A.D. and Zverev, V.G., "Mathematical Modelling of the Spreading of High-Level Forest Fires", Sov. Phys. Dokl., 28, 328-330, 1983.
- [3] Grishin, A.M., Gruzin, A.D. and Zverev V.G., "Study of the Structure and Limits of Propagation of the Front of an Upstream Forest Fire", Fizika Goreniya i Vzryva, 21:1, 11-21, 1985.
- [4] Zijlema, M, Segal, A. and Wesseling, P., "Finite Volume Computation of Incompressible Turbulent Flows in General Co-ordinates on Staggered Grids", Int. J. on Numerical Methods in Fluids, 20, 621-640, 1995.
- [5] Yakhot, V., Orszag, S., "Renormalization Group Analysis of Turbulence", J. of Sci. Computing, 1:1, 3-51, 1986.
- [6] Yakhot, V., Smith, M., "The Renormalization Group, the ε -Expansion and Derivation of Turbulence Models", J. of Sci. Computing, 7:1, 35-61, 1992.
- [7] Grishin, A.M., Zverev, V.G. and Shevelev, S.V., "Steady State Propagation of Top Crown Forest Fires", Fizika Goreniya i Vzryva, 22:6, 101-108, 1986.
- [8] Magnussen, B., Hjertager, H., "On Mathematical Modeling of Turbulent Combustion with Special Emphasis on Soot Formation and Combustion", in the *Proceedings of the 16th Int. Symp. on Combustion*, The Combustion Institute, pp. 719-729, 1976.
- [9] Kaplan, C., Shaddix, C.R. and Smyth, K.C., "Computations of Enhanced Soot Production in Time-Varying CH₄/air Diffusion Flames", Comb. and Flame, 106:4, 392-405, 1996.
- [10] Grishin, A.M., Mathematical Modeling of Forest Fires and New Methods of Fighting Them. Ed. by F. Albini, Publishing House of the Tomsk University, Russia, Tomsk, 1997.
- [11] Porterie, B., Morvan, D., Larini, M. and Loraud, J.C., "Wildfire Propagation: a Two Dimensional Multiphase Approach", Combust., Explosion and Shock Waves, 34:2, 139-150, 1998.
- [12] Fiveland, W.A., "Discrete Ordinate Methods for Radiative Heat Transfer in Isotropically and Anisotropically Scattering Media", ASME J. of Heat Transfer, 109, 809-812, 1987.
- [13] Lathrop, K.D., "Spatial Differencing of the Transport Equation: Positivity vs Accuracy", J. of Comp. Phys., 4, 475-498, 1969.
- [14] De Mestre, N.J., Catchpole, E.A. and Anderson, D.H., "Uniform Propagation of a Planar Fire Front Without Wind", Comb. Sci. and Techn., 65, 231-244, 1989.
- [15] Clift, R., Grace, J.R. and Weber M.E., Bubbles, Drops and Particles, Academic Press. New York, 1978.
- [16] Incropera, F.P., De Witt, D.P., Fundamentals of Heat and Mass Transfer, Wiley, New York, 1985.
- [17] Leonard, B.P., "The Ultimate Conservative Difference Scheme Applied to Unsteady One Dimensional Advection", Comp. Meth. Appl. Mech. Eng., 88, 17-74, 1991.
- [18] Patankar, S.V., Numerical Heat Transfer and Fluid Flow. Mc Graw Hill, New York, 1980.
- [19] Moss, J.B., "Turbulent Diffusion Flames". in Combustion Fundamentals of Fire Ed. Cox G., Academic Press, San Diego, CA, 1995.
- [20] Ventura, J., Mendes-Lopes, J.M. "Forest Fire Behaviour on Laboratory Rig". Intermediate confidential report Efaistos Project, 1998.

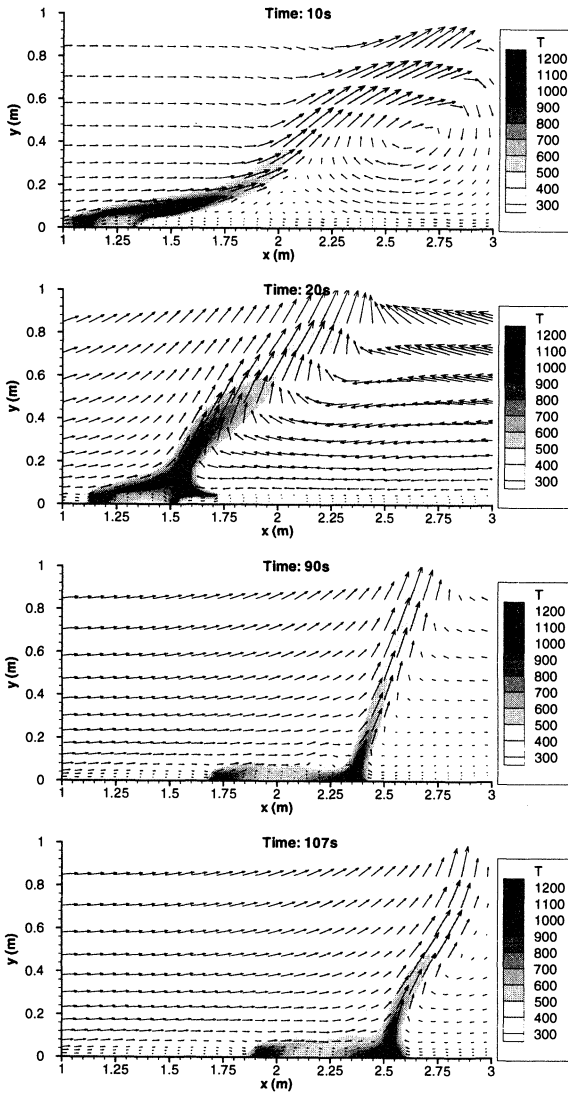


Figure 1: Fire spread in a bed of pine needles. The fuel bed is distributed from $x=1\text{m}$ to $x=3.2\text{m}$ over a depth of 0.05 m . Gas temperature field and velocity vector at different times for a wind speed of 1 m/s .

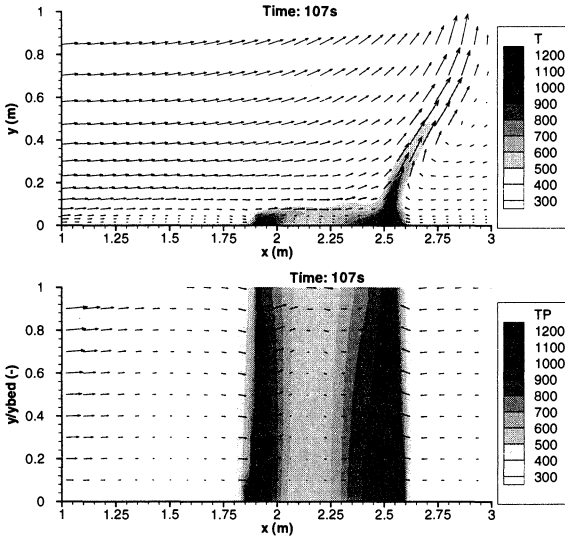


Figure 2: Fire spread in a bed of pine needles. Gas and solid phase temperature fields and velocity vector at $t=107s$ for a wind speed of 1 m/s. Note that y/y_{bed} corresponds to the nondimensional fuel bed height.

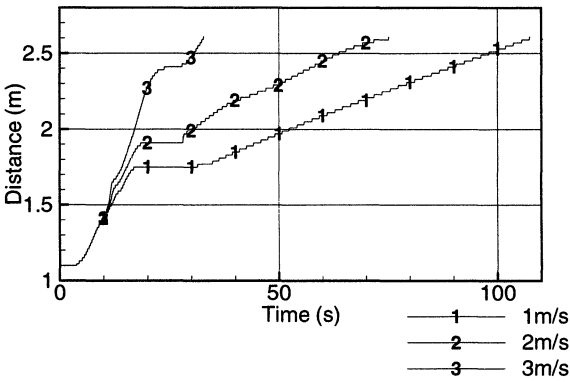


Figure 3: Predicted pyrolysis front trajectory for the three wind conditions.

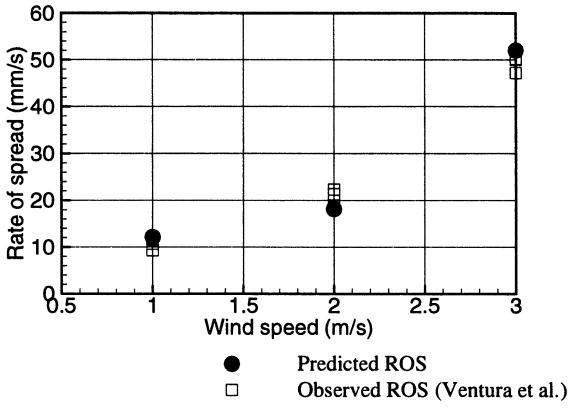


Figure 4: Predicted and measured rates of spread versus wind speed.